JACC: BASIC TO TRANSLATIONAL SCIENCE
VOL. 1, NO. 3, 2016
ISSN 2452-302X
http://dx.doi.org/10.1016/j.jacbts.2016.02.002

PRE-CLINICAL RESEARCH

Microtubule-Mediated Misregulation of Junctophilin-2 Underlies T-Tubule Disruptions and Calcium Mishandling in *mdx* Mice

Kurt W. Prins, MD, PhD,[a] Michelle L. Asp, PhD,[b] Huiliang Zhang, PhD,[c] Wang Wang, MD, PhD,[c] Joseph M. Metzger, PhD[b]

VISUAL ABSTRACT

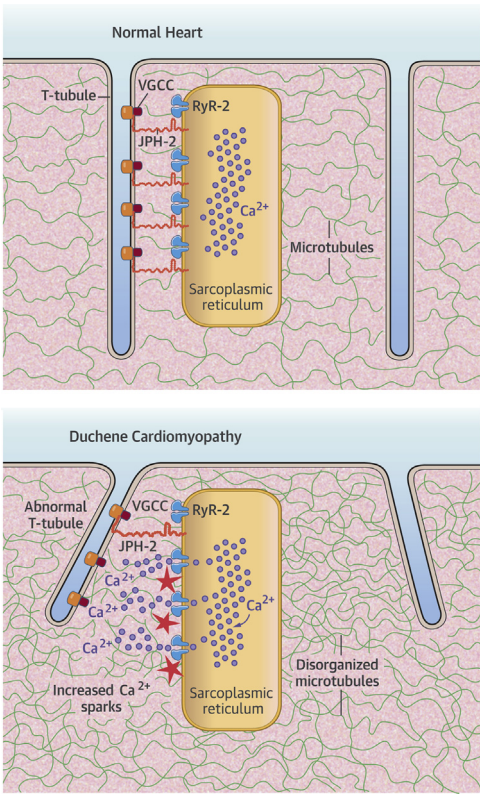

Prins, K.W. et al. J Am Coll Cardiol Basic Trans Science. 2016; 1(3):122–30.

HIGHLIGHTS

- **Decreased junctophilin-2 levels are associated with cardiac t-tubule derangements in *mdx* mice, the mouse model of Duchenne muscular dystrophy (DMD).**
- **Reduced junctophilin-2 protein levels correlate with increases in total microtubule content in *mdx* hearts.**
- **Colchicine-mediated microtubule depolymerization increases junctophilin-2 protein levels and improves localization patterns which, in turn, are associated with t-tubule reorganization and reduced calcium sparks.**
- **This study identifies microtubule-mediated misregulation of junctophilin-2 as a novel molecular mechanism in Duchenne cardiomyopathy.**

From the [a]Cardiovascular Division, University of Minnesota Medical School, Minneapolis, Minnesota; [b]Department of Integrative Biology and Physiology, University of Minnesota Medical School, Minneapolis, Minnesota; and the [c]Mitochondria and Metabolism Center, University of Washington, Seattle, Washington. This work was supported by the University of Minnesota Lillehei Heart Institute. Dr. Metzger has received grants from the National Institutes of Health (NIH) and MDA. Dr. Prins has received NIH T32 (HL069764) and F32 (HL129554) grants. Dr. Asp has received the NIH F32 (HL115876) grant. Dr. Wang has received the NIH RO1 (HL114760) grant. All other authors have reported that they have no relationships relevant to the contents of this paper to disclose.

Manuscript received January 14, 2016; revised manuscript received February 23, 2016, accepted February 23, 2016.

SUMMARY

Cardiac myocytes from the *mdx* mouse, the mouse model of Duchenne muscular dystrophy, exhibit t-tubule disarray and increased calcium sparks, but a unifying molecular mechanism has not been elucidated. Recently, improper trafficking of junctophilin (JPH)-2 on an altered microtubule network caused t-tubule derangements and calcium mishandling in a pressure-overload heart failure model. *Mdx* cardiac myocytes have microtubule abnormalities, but how this may affect JPH-2, t-tubules, and calcium handling has not been established. Here, we investigated the hypothesis that an inverse relationship between microtubules and JPH-2 underlies t-tubule disruptions and calcium mishandling in *mdx* cardiac myocytes. Confocal microscopy revealed t-tubule disorganization in *mdx* cardiac myocytes. Quantitative Western blot analysis demonstrated JPH-2 was decreased by 75% and showed an inverse hyperbolic relationship with α- and β-tubulin, the individual components of microtubules, in *mdx* hearts. Colchicine-induced microtubule depolymerization normalized JPH-2 protein levels and localization, corrected t-tubule architecture, and reduced calcium sparks. In summary, these results suggest microtubule-mediated misregulation of JPH-2 causes t-tubule derangements and altered calcium handling in *mdx* cardiac myocytes. (J Am Coll Cardiol Basic Trans Science 2016;1:122–30)

Loss of dystrophin causes Duchenne muscular dystrophy (DMD), an X-linked disease characterized by striated muscle dysfunction resulting in a life expectancy of only 20 years to 30 years (1). Heart failure is the cause of death for 20% to 25% of DMD patients (2); therefore research aimed at understanding the molecular and cellular phenotypes underlying the cardiomyopathy of DMD has been conducted. Altered calcium homeostasis marked by increased calcium sparks (3–5) and t-tubule disarray were documented in cardiac myocytes from the dystrophin-deficient *mdx* mouse (6,7), but a unifying molecular mechanism has not been identified.

Junctophilin (JPH)-2, the protein that links the plasma membrane of t-tubules to the ryanodine receptor, is essential for proper t-tubule structure and function (8). Recently, it was reported that JPH-2 mislocalization due to abnormalities in microtubule cytoskeleton caused pathological t-tubule remodeling and abnormal calcium handling in the pressure overload-induced heart failure model (9). However, the relationship between microtubules and JPH-2 in other models of heart failure or cardiomyopathy has not been analyzed. Because previous studies documented microtubule derangements in *mdx* cardiac myocytes (5,10), we tested the hypothesis that microtubule alterations cause JPH-2 misregulation and result in t-tubule disruptions and calcium mishandling in *mdx* mice.

Finally, to investigate the translational aspects of our hypothesis, we examined the cardiomyopathy of *mdx* mice via echocardiography and isoproterenol stress tests as previous studies showed mildly reduced systolic function (11–14) and excessive mortality with isoproterenol administration (10,15,16) in *mdx* mice. Because Zhang et al. (9) and Guo et al. (17) showed improvement in systolic function with normalization of JPH-2, we hypothesized colchicine-induced JPH-2 normalization would reduce the severity of *mdx* cardiomyopathy.

METHODS

MICE. Control C57BL/10 and *mdx* mice were purchased from Jackson Laboratories. All animals were housed and treated following the guidelines set forth by the University of Minnesota Institutional Animal Care and Use Committee.

ANTIBODIES. Polyclonal antibodies for voltage-gated calcium channel (VGCC) (Sigma, Waltham, Massachusetts) and JPH-2 (ThermoScientific) and monoclonal antibodies for α-tubulin (Sigma), β-tubulin (Sigma), and dystrophin (Leica, Buffalo Grove, Illinois) were purchased from the identified vendors. Alexa-Fluor-488 or Alexa-Fluor-568–conjugated anti-rabbit antibodies were purchased from Molecular Probes (Eugene, Oregon). Infrared dye-conjugated anti-mouse and anti-rabbit antibodies were purchased from LICOR Biosciences (Lincoln, Nebraska).

ISOLATION OF CARDIAC MYOCYTES. Isolation of ventricular cardiac myocytes was performed as described previously (18).

T-TUBULE ASSESSMENT. Freshly isolated cardiac myocytes were fixed in 4% paraformaldehyde for 10 min at 37°C, washed with phosphate-buffered saline (PBS) 2 times for 5 min, incubated with AlexaFluor 488

ABBREVIATIONS AND ACRONYMS

DMD = Duchenne muscular dystrophy

JPH-2 = junctophilin-2

PBS = phosphate-buffered saline

SR = Sarcoplasmic reticulum

TT = transverse tubules

VGCC = voltage-gated calcium channel

WT = wild-type

conjugated Wheat Germ Agglutinin (Sigma) for 10 min at room temperature, and then washed in PBS 2 times for 5 min. Cells were mounted in Antifade (Molecular Probes) and imaged on Bio-Rad MRC 1000 scan head mounted on an upright Nikon Optishot microscope (Tokyo, Japan) at the University Imaging Centers at the University of Minnesota. Z-stacks were collected and converted into a z-projection using ImageJ (Bethesda, Maryland). T-tubule quantification was performed using the TT_{Power} plugin on ImageJ as described (7).

IMMUNOFLUORESCENCE ANALYSIS. Primary cardiac myocytes were fixed in 4% paraformaldehyde for 10 min at 37°C, permeabilized with 1% Triton X-100 (Sigma) in PBS, blocked in 5% BSA for 10 min 3 times, and incubated with primary antibodies overnight at 4°C. Sections were then washed and blocked with 5% bovine serum albumin for 10 min 3 times and then incubated with Alexa-Fluor-488- or Alexa-Fluor-568–conjugated secondary antibodies for 30 min at 37°C. Then, cardiac myocytes were washed with PBS and mounted in Anti-Fade Reagent (Molecular Probes).

CALCIUM TRANSIENT MEASUREMENTS. Freshly isolated cardiac myocytes were loaded with Fura-2AM (a ratiometric Ca^{2+} indicator; 2 μM [Molecular Probes]) for 10 min at room temperature after a de-esterification period of 20 min in M199 medium (Sigma). Cells were incubated with 10 μm colchicine or vehicle (double-distilled water [ddH_2O]) for 2 h and then subjected to calcium analysis. Fura-2 fluorescence was measured using a spectrophotometer (Stepper Switch, IonOptix). Initially, Fura-2 was excited at 360 nm (the isosbestic point independent of Ca^{2+}) and then continuously at 380 nm (Ca^{2+}-dependent fluorescence). Emission was collected at >510 nm by a photomultiplier tube. Ratiometric data were collected and analyzed online using commercial software (IonOptix).

CALCIUM SPARK ANALYSIS. Freshly isolated adult cardiac myocytes were plated on glass coverslips coated with 10 μg/ml laminin and in M199 medium and allowed to attach for 2 h. Then, colchicine (10 μM) or vehicle was added for 2 h. Cardiac myocytes were loaded with Ca^{2+} indicator Fluo 8-AM (5 μM, AAT Bioquest, Sunnyvale, California) for 10 min at room temperature followed by washout. For confocal imaging, we used an inverted confocal microscope (Leica TCS SP8, Wetzlar, Germany) with a 40×, 1.3 NA oil-immersion objective. Fluo 8-AM was excited at 488 nm and the emission was collected at >505 nm. For Ca^{2+}spark imaging, line scan was performed at a speed of 1.43 ms/line for 1,000 lines.

SARCOPLASMIC RETICULUM LOAD ANALYSIS. Freshly isolated cardiac myocytes plated on laminin-coated coverslips were treated with 10 μM colchicine or vehicle for 2 h and were then loaded with 2 μM Fura-2AM for 10 min and de-esterified for 10 min at room temperature. After de-esterification, coverslips were mounted onto a perfusion chamber and perfused with modified Tyrode's solution (in mM: 140 NaCl, 0.5 $MgCl_2$, 5 HEPES, 5.5 glucose, 1.8 $CaCl_2$, 5 KCl; pH 7.4) at 30°C. Myocytes were paced at 0.5 Hz for at least 20 s after which pacing was stopped and the perfusate was switched to Tyrode's solution with 20 mM caffeine to measure the sarcoplasmic reticulum calcium load. Finally, myocytes were again perfused with Tyrode's solution and paced at 0.5 Hz to ensure they were still viable. No more than 2 myocytes were measured per coverslip. Transient data were collected by measuring the 360:380 ratio using the Ionoptix Calcium and Contractility System and data were analyzed using IonWizard software (Westwood, Massachusetts).

IMAGE PROCESSING. Confocal images were collected and equivalently processed using Adobe Photoshop Version CS6 (San Jose, California).

WESTERN BLOT ANALYSIS AND QUANTIFICATION. Whole protein extracts from isolated ventricles from mice were performed as described (19). Protein concentration was determined using a BCA protein assay kit (Pierce, Waltham, Massachusetts). Cardiac extracts (25 μg) were subjected to sodium dodecyl sulfate–polyacrylamide gel electrophoresis (SDS-PAGE) and then transferred to nitrocellulose membrane. Membranes were washed/blocked in 5% milk in PBS for 1 h, and incubated with primary antibodies for 1 h at room temperature. Membranes were then washed/blocked twice for 10 min in 5% milk in PBS and then incubated with infrared secondary antibodies for 30 min at room temperature. Membranes were washed in Tris-buffered saline containing 0.1% Tween (Sigma) twice for 5 min. Imaging and quantification of Western blots was performed on an Odyssey Infrared Imaging system. SDS-PAGE was performed in parallel and stained with Coomassie brilliant blue stain and was imaging at the 700 nm wavelength on the Odyssey Imaging system (Lincoln, Nebraska) to serve as the loading control as described (20).

CHRONIC COLCHICINE TREATMENT. Mice were treated with intraperitoneal injection of either filter-sterilized PBS or 0.5 mg/kg of filter-sterilized colchicine (Sigma) dissolved in PBS every other day for 2 weeks.

ECHOCARDIOGRAPHY. Echocardiographic analysis was conducted using a VisualSonics 2100 ultrasound machine (Toronto, Ontario, Canada) with mice anesthetized with 2% to 3% inhaled isoflurane. Heart rate had to be >400 beats/min during echocardiographic

FIGURE 1 T-Tubule Derangements in *mdx* Mice Are Associated With JPH-2 Misregulation

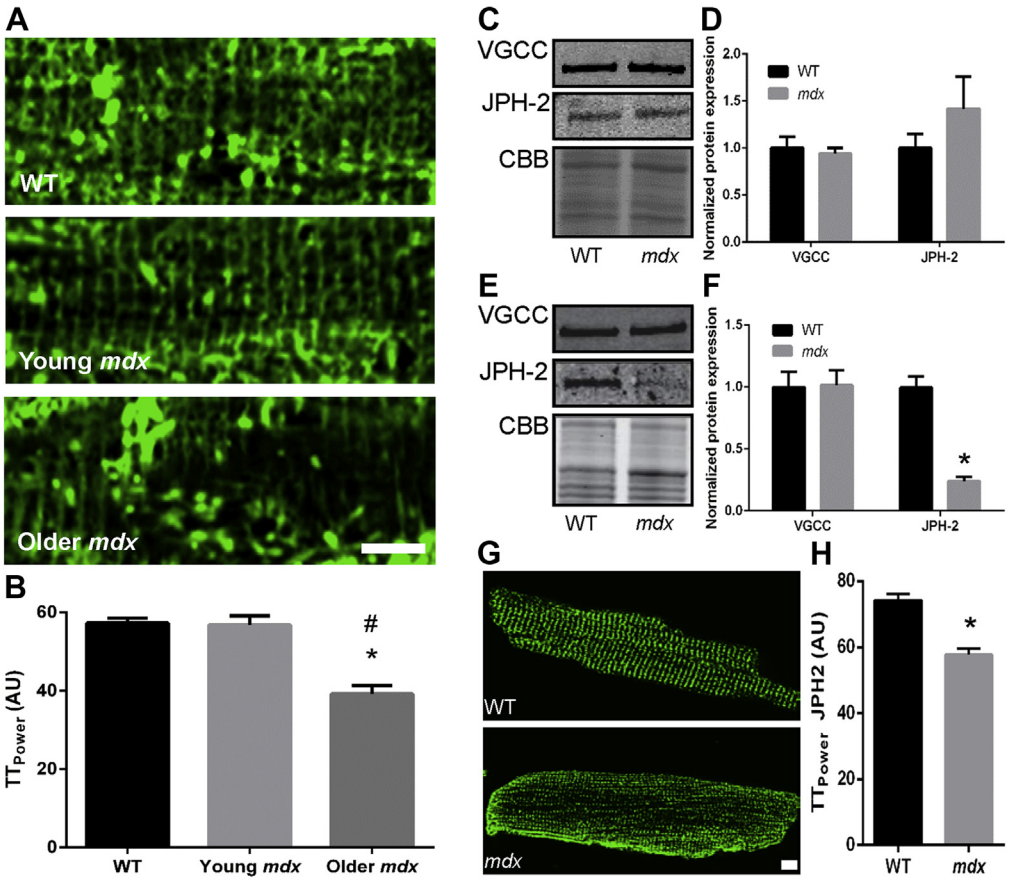

(A) Representative confocal images of cardiac myocytes stained with wheat germ agglutinin to delineate t-tubules. Older (8 months to 10 months) but not young (2 months to 3 months) *mdx* mice showed loss of regularity of the t-tubule network. Scale bar equals 5 μm. **(B)** Quantification of t-tubule organization in older (8 months to 10 months of age) WT, young, and older *mdx* mice. There was a significant reduction in t-tubule regularity in aged *mdx* mice. An asterisk **(*)** indicates $p \leq 0.05$ when compared to WT; A pound symbol **(#)** indicates $p \leq 0.05$ when compared to young *mdx* as determined by 1-way ANOVA with Tukey post-hoc analysis. N = 17 cells to 20 cells per genotype from 2 animals to 3 animals per genotype. Representative Western blot analyses and subsequent quantification from cardiac extracts of young (ages 2 months to 3 months) **(C and D)** and older (8 months to 10 months) **(E and F)** WT and *mdx* mice along with CBB stained SDS-PAGE, which served as a loading control. There was no difference in VGCC but there was a significant 75% reduction in JPH-2 levels in older *mdx* mice ($p = 0.0003$). N = 3 animals to 4 animals per genotype per age. **(G)** Representative confocal micrographs of cardiac myocytes from aged-matched (8 months to 10 months) control and *mdx* cardiac myocytes stained for JPH-2. Scale bar equals 5 μm. **(H)** Quantification of JPH-2 localization using TT_{Power}. Older *mdx* mice showed altered localization of JPH-2 in cardiac myocytes ($p < 0.0001$). N =17 cells to 19 cells from 2 animals to 3 animals per treatment. An asterisk **(*)** indicates $p \leq 0.05$ as determined using Student *t* test. Values are presented as mean ± SEM. ANOVA = analysis of variance; CBB = Coomassie brilliant blue; JPH-2 = junctophilin-2; SDS-PAGE = sodium dodecyl sulfate–polyacrylamide gel electrophoresis; VGCC = voltage-gated calcium channel; WT = wild-type.

analysis. Systolic and diastolic dimensions and fractional shortening were determined from M-mode images in the parasternal short-axis view at the level of the mitral valve.

ISOPROTERENOL STRESS TESTS. Eight-month to 10-month-old wild-type (WT) and *mdx* mice (n = 8 mice to 10 mice per treatment group) were treated with either PBS or colchicine for 2 weeks and then administered isoproterenol at a dose 10 mg/kg at 9AM, 1PM, and 5PM via intraperitoneal injection for 3 consecutive days. Survival was assessed at 8-h intervals for the first 5 days and then daily thereafter.

STATISTICAL ANALYSIS. All data are represented as mean ± standard error of the mean. Student *t* tests were used to compare 2 groups with assumed equivalent variance if sample size was <5 with an F-test to assess variance if sample size was >5 and 1-way

FIGURE 2 Negative Hyperbolic Relationship Between JPH-2 and Tubulin in Aged *mdx* Cardiac Extracts

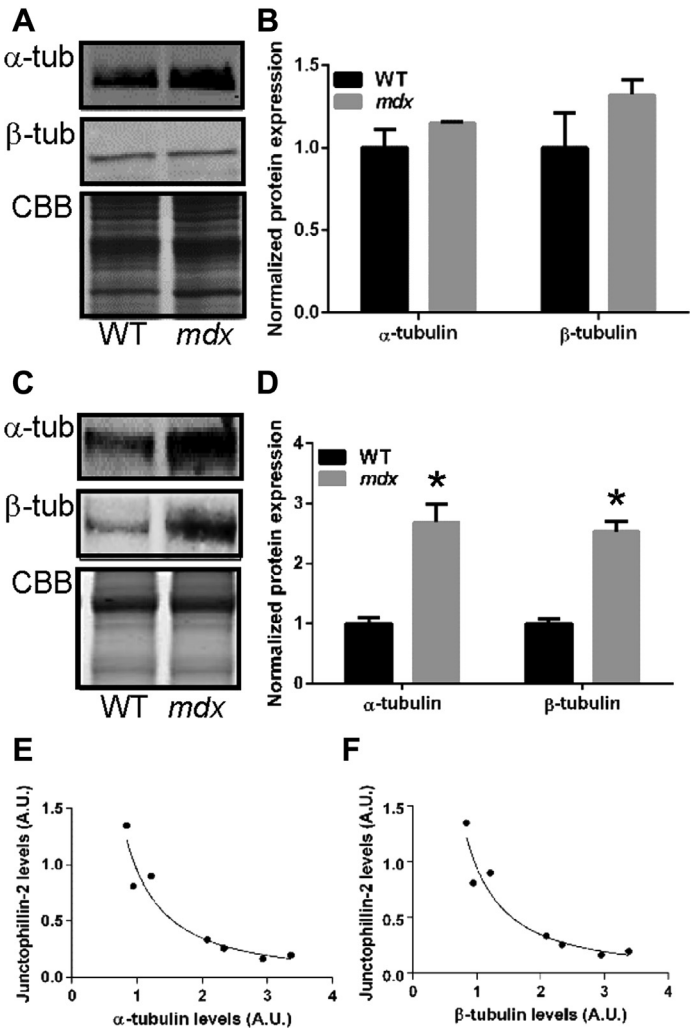

Quantitative Western blot analysis of α- and β-tubulin levels in young **(A and B)** and aged **(C and D)** *mdx* mice. There was no significant difference in tubulin levels in young (2 months to 3 months of age) mice but older (8 months to 10 months of age) *mdx* mice showed a significant 2.6-fold increase in α- and β-tubulin protein expression. (For α-tubulin comparison, $p = 0.0008$. For β-tubulin comparison, $p = 0.0007$.) N = 3 animals to 4 animals per genotype per age point. **(E and F)** A strong negative hyperbolic relation between JPH-2 and α- and β-tubulin in older *mdx* cardiac extracts exists ($r^2 = 0.95$ for α-tub and JPH-2 curve-fitting, and $r^2 = 0.95$ for β-tubulin and JPH-2 curve fitting). *$p \leq 0.05$ as determined using Student *t* test. Values are presented as mean ± SEM. Abbreviations as in Figure 1.

analysis of variance with Tukey post-hoc test was used to compare means between 3 groups. Kaplan-Meier survival curve was used to determine survival differences after initial treatment with isoproterenol with log-rank test to assess differences in survival. Statistical significance was defined as $p \leq 0.05$.

RESULTS

T-TUBULE DISRUPTIONS IN *mdx* CARDIAC MYOCYTES ARE ASSOCIATED WITH REDUCED JPH-2 PROTEIN LEVELS AND ALTERED LOCALIZATION. We first analyzed the t-tubule network in isolated cardiac myocytes from young (2- to 3-months old) and older (8- to 10-months old) WT and *mdx* mice. The 8- to 10-month time was used because that is the age when *mdx* mice begin to show signs of cardiomyopathy (12,14). When compared to 8-month to 10-months of age, WT and young *mdx* cardiac myocytes had no discernable difference in t-tubule architecture, but older *mdx* cardiac myocytes showed disrupted t-tubules (Figure 1A). When quantified using TT_{Power} analysis, older *mdx* t-tubule structural integrity (39.2 ± 2.2 AU) was significantly different than WT (57.3 ± 1.3 AU) and young *mdx* mice (56.8 ± 2.3 AU) (Figure 1B).

To provide insight into the mechanism of t-tubule disruptions in older *mdx* mice, we investigated 2 key t-tubule proteins: the VGCC and JPH-2. Protein levels of VGCC were not altered in either young or older *mdx* heart extracts (Figures 1C to 1F). However, JPH-2 protein levels were markedly reduced by 75% in older *mdx* hearts (WT: 1 ± 0.9 AU and *mdx*: 0.024 ± 0.4 AU) but not significantly altered in young mice (WT: 1.0 ± 0.1 AU and *mdx*: 1.3 ± 0.2 AU) (Figures 1C to 1F), a pattern that mirrored the t-tubule phenotype. Immunofluorescence analysis of isolated cardiac myocytes from older WT (74.2 ± 1.9 AU) and *mdx* mice (57.8 ± 1.7 AU) revealed altered localization of JPH-2 in *mdx* mice (Figures 1G and 1H). In summary, JPH-2 misregulation was associated with t-tubule disruptions in *mdx* hearts.

INVERSE HYPERBOLIC RELATIONSHIP BETWEEN JPH-2 AND α- AND β-TUBULIN. Because a previous report demonstrated that an altered microtubule cytoskeleton caused mislocalization of JPH-2 (9), we analyzed the relationship between α- and β-tubulin, the individual components of microtubules, and JPH-2 in *mdx* hearts. At a young age when JPH-2 levels were normal, α-tubulin (WT: 1.0 ± 0.1 AU and *mdx*: 1.2 ± 0.1 AU) and β-tubulin (WT: 1.0 ± 0.2 AU and *mdx*: 1.3 ± 0.1 AU) protein expression was not significantly different in *mdx* cardiac extracts (Figures 2A and 2B). However, in older *mdx* hearts when JPH-2 protein was reduced, α-tubulin (WT: 1.0 ± 0.1 AU and *mdx*: 2.7 ± 0.3 AU) and β-tubulin (WT: 1.0 ± 0.9 AU and *mdx*: 2.5 ± 0.2 AU) content was increased approximately 2.6-fold (Figures 2C and 2D). When the relationships between α- and β-tubulin and JPH-2 in older mice was analyzed, we observed a significant inverse hyperbolic relationships ($r^2 = 0.95$

for both curve fitting models) (Figures 2E and 2F). These data suggested increased microtubule content was associated with reduced JPH-2 protein levels.

COLCHICINE-INDUCED MICROTUBULE DEPOLYMERIZATION NORMALIZED JPH-2 LEVELS AND LOCALIZATION WHICH CORRECTED T-TUBULE MORPHOLOGY IN *mdx* MICE. To further probe the relationship between microtubules and JPH-2 in *mdx* hearts, we treated older *mdx* mice for 2 weeks with colchicine to induce microtubule depolymerization and examined the effects on JPH-2 and t-tubules. Colchicine treatment effectively depolymerized microtubules in cardiac myocytes in vivo (Figure 3A) and was associated with a 7.6-fold increase in JPH-2 protein levels (*mdx*-PBS: 1.0 ± 0.08 AU and *mdx*-colchicine: 7.6 ± 1.0 AU) (Figures 3B and 3C). Moreover, JPH-2 localization patterns in *mdx* cardiac myocytes were significantly improved with colchicine treatment (*mdx*-PBS: 62.6 ± 1.6 AU and *mdx*-colchicine: 68.1 ± 1.9 AU) (Figure 3D and 3E). Finally, colchicine-mediated restoration of JPH-2 improved t-tubule organization in older *mdx* hearts (*mdx*-PBS: 44.5 ± 2.0 AU and *mdx*-colchicine: 52.5 ± 2.2 AU) (Figures 3F and 3G).

ACUTE COLCHICINE TREATMENT IMPROVED CALCIUM HANDLING IN *mdx* CARDIAC MYOCYTES. Because JPH-2 was shown to be an important regulator of the ryanodine receptor (21–23), we investigated how colchicine-mediated JPH-2 restoration affected calcium handling in isolated *mdx* cardiac myocytes treated acutely with colchicine. Acute colchicine treatment did not affect diastolic calcium, onset kinetics, or amplitude of calcium transients, but there was accelerated calcium decay at 25% to baseline (*mdx*: 59.4 ± 2.5 ms and *mdx*-colchicine: 51.1 ± 3.0 ms) but not at 75% to baseline (*mdx*: 219.9 ± 20.4 ms and *mdx*-colchicine: 202.2 ± 25.0 ms) (Figures 4A to 4F), which suggested improved ryanodine receptor gating. To further investigate ryanodine receptor activity, we measured calcium spark frequency and found acute colchicine treatment reduced calcium sparks by more than 50% (*mdx*: 0.84 ± 0.2 sparks/s/100 μm and *mdx*-colchicine: 0.31 ± 0.08 sparks/s/100 μm) (Figures 4G and 4H). Acute colchicine treatment caused a nonsignificant alteration in sarcoplasmic reticulum calcium load (Supplemental Figure 1), which would not explain the reduction in calcium sparks. All together, these data suggest that acute colchicine treatment improved ryanodine receptor gating in *mdx* cardiac myocytes.

CHRONIC COLCHICINE TREATMENT DID NOT ALTER ORGAN-LEVEL ASSESSMENTS OF CARDIOMYOPATHY IN *mdx* MICE. Next, we determined if 2 weeks of colchicine treatment led to whole-organ level improvements in older *mdx* mice. M-mode echocardiography did not reveal any significant changes in cardiac geometry or systolic function after 2 weeks of colchicine treatment in *mdx* mice (Supplemental Figure 2), but both *mdx*

FIGURE 3 Microtubule Depolymerization Normalized JPH-2 Levels and Localization and t-Tubule Morphology in *mdx* Mice

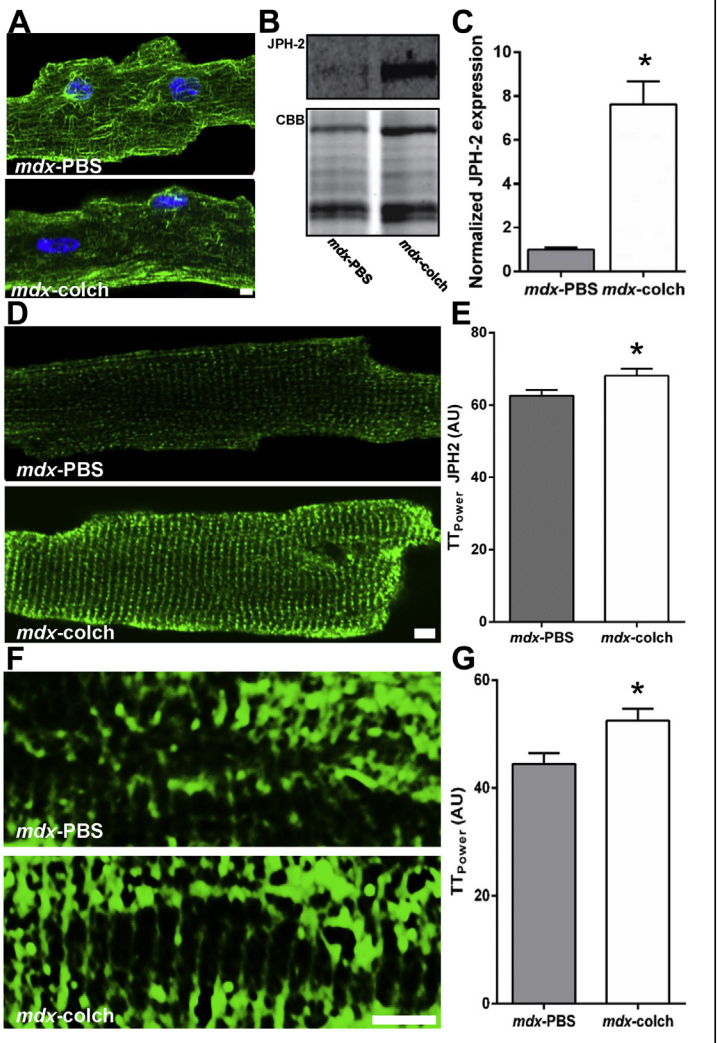

(A) Confocal micrographs of cardiac myocytes stained with an α-tubulin antibody to show the microtubule cytoskeleton. Colchicine depolymerized microtubule in vivo. **(B)** Representative Western blots and CBB-stained SDS-PAGE of extracts from *mdx* mice treated with either PBS or colchicine. **(C)** JPH-2 was upregulated 7.6-fold in mice treated with colchicine ($p = 0.0007$). **(D)** Representative confocal micrographs showing JPH-2 levels and localization. **(E)** Quantification of JPH-2 localization using TT_{Power}. JPH-2 localization improved with colchicine treatment ($p = 0.04$). N = 20 cells to 22 cells from 2 animals to 3 animals per treatment. **(F)** Representative images of t-tubules stained with wheat germ agglutinin from cardiac myocytes isolated from *mdx* treated with either PBS or colchicine. **(G)** Quantification of t-tubule organization using TT_{Power}. Colchicine resulted in a significant improvement in t-tubule organization ($p = 0.02$). N = 19 cells to 20 cells per treatment from 2 animals to 3 animals. An asterisk **(*)** indicates $p \leq 0.05$ as determined using Student *t* test. Scale bar is 5 μm in all images. Values are presented as mean ± SEM. PBS = phosphate-buffered saline; other abbreviations as in Figure 1.

FIGURE 4 Colchicine Treatment Improved Calcium Handling in *mdx* Cardiac Myocytes

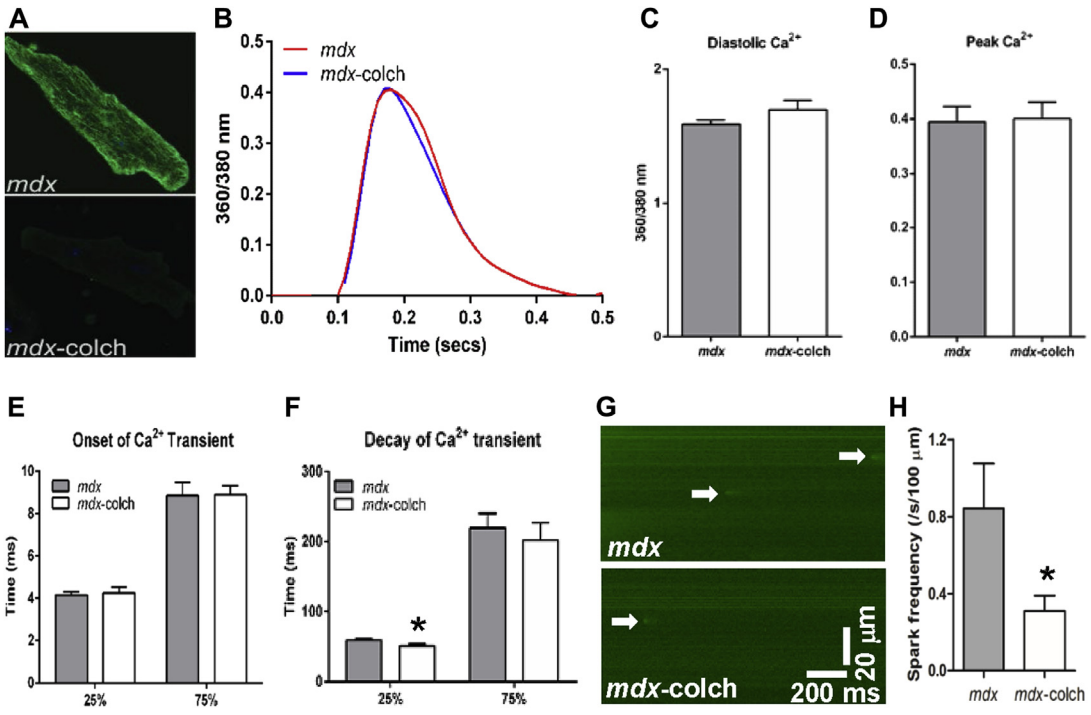

(A) Confocal micrographs of *mdx* cardiac myocytes stained with an α-tubulin antibody to show effective microtubule depolymerization with colchicine treatment. **(B)** Representative curves of calcium transients. **(C–E)** Colchicine treatment did not affect baseline calcium, peak calcium, or kinetics of onset of calcium transients, but increased calcium transient decay to 25% of baseline calcium levels ($p = 0.03$). **(F)**. $N = 20$ cells to 22 cells from 2 animals to 3 animals per treatment. **(G)** Representative calcium spark images from isolated *mdx* cardiac myocytes. **Arrows** indicate calcium sparks. **(H)** Quantification of calcium sparks frequency. Colchicine treatment significantly reduced calcium sparks in *mdx* cardiac myocytes ($p = 0.04$). $N = 17$ cells to 20 cells from 3 animals per treatment. *$p \leq 0.05$ as determined by Student *t* test. Values are presented as mean ± SEM.

groups showed signs of mild cardiomyopathy when compared to age-matched WT mice. Finally, colchicine treatment did not confer a significant survival benefit when older *mdx* mice were subjected to isoproterenol stress test (WT survival: 75%, *mdx*-colchicine survival: 40%, *mdx*-PBS survival: 10%) (Supplemental Figure 3).

DISCUSSION

Our main new findings are the following: 1) t-tubule disarray in *mdx* cardiac myocytes is associated with altered localization and decreased protein levels of JPH-2; 2) there is a significant inverse hyperbolic relationship between JPH-2 and α- and β-tubulin, the individual subunits of microtubules, in *mdx* hearts; 3) disruption of the JPH-2/microtubule relationship, using colchicine to depolymerize microtubules, not only normalizes JPH-2 localization, but we show for the first time that it restores JPH-2 protein levels which corrects t-tubule morphology; and 4) colchicine treatment can effectively reduce calcium spark frequency in isolated *mdx* cardiac myocytes, which we propose is mediated through stabilization of the ryanodine receptor. Collectively, these results provide evidence that microtubule-dependent misregulation of JPH-2 underlies t-tubule derangements and abnormal calcium handling in Duchenne cardiomyopathy, and implicates JPH-2 as a new molecular mediator in the pathophysiology of Duchenne cardiomyopathy.

Importantly, our results provide additional mechanistic insight into 2 secondary pathological cardiac phenotypes associated with dystrophin-deficiency: t-tubule disruptions and calcium mishandling. First of all, we show that normalization of JPH-2 protein levels and localization improves t-tubule architecture, a cellular phenotype that has not had a proposed molecular mechanism.

Secondly, colchicine treatment reduces calcium spark frequency which was in agreement with results of Kerr et al. (24), which we propose is due to normalization of JPH-2 after microtubule depolymerization leading to improved ryanodine receptor gating. These results provide an additional molecular mechanism by which the ryanodine receptor gating is altered in *mdx* cardiac myocytes, in addition to the loss of a calstabin-ryanodine receptor interaction as previously defined (4). In summary, our results implicate JPH-2 as the molecular mediator of t-tubule abnormalities and abnormal gating of the ryanodine receptor in Duchenne cardiomyopathy.

Next, we provide further support for the hypothesis that JPH-2 regulates ryanodine receptor activity. Several studies have documented increased calcium spark frequency when JPH-2 is decreased or altered in localization (9,21–23), suggesting the ryanodine receptor is improperly gated when JPH-2 is disrupted. In particular, Zhang et al. (9) showed that microtubule depolymerization-induced normalization of JPH-2 localization patterns reduced calcium spark frequency in cultured mouse cardiac myocytes, a result very similar to our findings. However, unlike Zhang et al. (9), we did not observe changes in calcium transient amplitude with colchicine treatment. The discrepancy between our results and those of Zhang et al. (9) may be due in-part to SR load as JPH-2 knockdown causes reduced SR calcium content, but calcium transients normalized to SR load are actually increased (22). *Mdx* mice have normal SR calcium content (25) and are not significantly altered by colchicine treatment (Supplemental Figure 1), which might explain why colchicine treatment did not increase calcium transient amplitude in *mdx* cardiac myocytes. Another explanation for the differences between our results and those of Zhang et al. (9) could relate to the timing of experiments as we analyzed calcium transients in freshly isolated cardiac myocytes whereas Zhang et al. (9) showed normalization of calcium transients in cells cultured for >48 h. Nonetheless, our results support a crucial role for JPH-2 in regulating ryanodine receptor activity.

Although we were able to document restoration of t-tubule organization with colchicine treatment, we did not observe organ-level cardiac improvements in *mdx* mice. One explanation is that t-tubule corrections do not always lead to improved whole organ function; a finding that was documented in previous publications. Firstly, t-tubule derangements precede left ventricular dysfunction in the thoracic aortic banded rat model (26). Moreover, while transgenic overexpression of JPH-2 could prevent pathological t-tubule remodeling and blunted the effects of aortic banding; it did not completely prevent the onset of heart failure (17). Another reason for the lack of improvement of cardiomyopathy in *mdx* mice treated with colchicine could be the relatively mild cardiomyopathy of *mdx* mice. Whereas Guo et al. (17) showed improvements in ejection fraction with JPH-2 overexpression, there was not a complete normalization of ejection fraction, which could explain why echocardiography did not reveal improvements in *mdx* mice treated with colchicine as the *mdx* mice had only mild reduced fractional shortening (Supplemental Figure 2). Finally, the lack of a significant improvement in isoproterenol stress test may be explained by the underlying pathophysiology that was corrected with colchicine treatment. Previously, membrane permeability was associated with increased death in *mdx* mice when treated with isoproterenol (10,15,16), and thus the nonsignificant improvement in survival with colchicine may have resulted from an inability to correct cardiac myocytes permeability in *mdx* hearts. In summary, there may be several reasons why colchicine treatment did not improve *mdx* cardiomyopathy.

Finally, our results add to several other publications that document a crucial role for JPH-2 in t-tubule integrity. The first link between JPH-2 and t-tubules was shown when knockout of JPH-2 resulted in embryonic lethality due to lack and cardiac contractility and improper t-tubule formation (27). Several other studies document that alterations of JPH-2 via miR-24 (28,29), RNA interference (21,22,30), or calpain-mediated protein cleavage (23) cause t-tubule derangements and rescue of JPH-2 protein levels or localization via transgenic overexpression (17), inhibition of miR-24 (28), calpain-inhibition (23), or microtubule depolymerization (9) prevent pathological t-tubule remodeling. Taken together with our new findings, JPH-2 is a critical mediator of t-tubule structure in cardiac myocytes.

ACKNOWLEDGEMENTS The authors would like to thank Drs. Amit Gaggar and Thenappan Thenappan for assistance in editing the manuscript.

REPRINT REQUESTS AND CORRESPONDENCE: Dr. Joseph M. Metzger, Department of Integrative Biology and Physiology, University of Minnesota, 321 Church Street SE, Minneapolis, Minnesota 55455. E-mail: metzgerj@umn.edu.

PERSPECTIVES

COMPETENCY IN MEDICAL KNOWLEDGE: Cardiomyopathy accounts for approximately one-quarter of deaths in Duchenne muscular dystrophy. Currently, our knowledge of the mechanistic pathophysiology of the Duchenne cardiomyopathy is incomplete, but these data provide a molecular explanation for the disruption of t-tubules and calcium mishandling in Duchenne cardiomyopathy.

TRANSLATIONAL OUTLOOK: Future studies that examine the effects of normalization of JPH-2 through multiple mechanisms including colchicine treatment, gene transfer, or micro-RNA inhibition in large animal models of Duchenne cardiomyopathy with a more severe phenotype could be conducted to gain further information about how JPH-2 affects outcomes in Duchenne cardiomyopathy. If results are positive, a clinical trial examining the effects of colchicine in Duchenne muscular dystrophy could be considered.

REFERENCES

1. Moser H. Duchenne muscular dystrophy: pathogenetic aspects and genetic prevention. Hum Genet 1984;66:17–40.

2. Fayssoil A, Nardi O, Orlikowski D, Annane D. Cardiomyopathy in duchenne muscular dystrophy: pathogenesis and therapeutics. Heart Fail Rev 2010;15:103–7.

3. Wang X, Weisleder N, Collet C, et al. Uncontrolled calcium sparks act as a dystrophic signal for mammalian skeletal muscle. Nat Cell Biol 2005;7:525–30.

4. Fauconnier J, Thireau J, Reiken S, et al. Leaky RyR2 trigger ventricular arrhythmias in duchenne muscular dystrophy. Proc Natl Acad Sci U S A 2010;107:1559–64.

5. Prosser BL, Ward CW, Lederer WJ. X-ROS signaling: rapid mechano-chemo transduction in heart. Science 2011;333:1440–5.

6. Lorin C, Gueffier M, Bois P, Faivre JF, Cognard C, Sebille S. Ultrastructural and functional alterations of EC coupling elements in mdx cardiomyocytes: an analysis from membrane surface to depth. Cell Biochem Biophys 2013;66:723–36.

7. Pasqualin C, Gannier F, Malecot CO, Bredeloux P, Maupoil V. Automatic quantitative analysis of t-tubule organization in cardiac myocytes using ImageJ. Am J Physiol Cell Physiol 2015;308:C237–45.

8. Landstrom AP, Beavers DL, Wehrens XH. The junctophilin family of proteins: from bench to bedside. Trends Mol Med 2014;20:353–62.

9. Zhang C, Chen B, Guo A, et al. Microtubule-mediated defects in junctophilin-2 trafficking contribute to myocyte transverse-tubule remodeling and Ca2+ handling dysfunction in heart failure. Circulation 2014;129:1742–50.

10. Strakova J, Dean JD, Sharpe KM, Meyers TA, Odom GL, Townsend D. Dystrobrevin increases dystrophin's binding to the dystrophin-glycoprotein complex and provides protection during cardiac stress. J Mol Cell Cardiol 2014;76C:106–15.

11. Adamo CM, Dai DF, Percival JM, et al. Sildenafil reverses cardiac dysfunction in the mdx mouse model of duchenne muscular dystrophy. Proc Natl Acad Sci U S A 2010;107:19079–83.

12. Quinlan JG, Hahn HS, Wong BL, Lorenz JN, Wenisch AS, Levin LS. Evolution of the mdx mouse cardiomyopathy: physiological and morphological findings. Neuromuscul Disord 2004;14:491–6.

13. Sarma S, Li N, van Oort RJ, Reynolds C, Skapura DG, Wehrens XH. Genetic inhibition of PKA phosphorylation of RyR2 prevents dystrophic cardiomyopathy. Proc Natl Acad Sci U S A 2010;107:13165–70.

14. Van Erp C, Loch D, Laws N, Trebbin A, Hoey AJ. Timeline of cardiac dystrophy in 3-18-month-old MDX mice. Muscle Nerve 2010;42:504–13.

15. Danialou G, Comtois AS, Dudley R, et al. Dystrophin-deficient cardiomyocytes are abnormally vulnerable to mechanical stress-induced contractile failure and injury. FASEB J 2001;15:1655–7.

16. Barnabei MS, Sjaastad FV, Townsend D, Bedada FB, Metzger JM. Severe dystrophic cardiomyopathy caused by the enteroviral protease 2A-mediated C-terminal dystrophin cleavage fragment. Sci Transl Med 2015;7:294ra106.

17. Guo A, Zhang X, Iyer VR, et al. Overexpression of junctophilin-2 does not enhance baseline function but attenuates heart failure development after cardiac stress. Proc Natl Acad Sci U S A 2014;111:12240–5.

18. Wang W, Barnabei MS, Asp ML, et al. Noncanonical EF-hand motif strategically delays Ca2+ buffering to enhance cardiac performance. Nat Med 2013;19:305–12.

19. Hanft LM, Rybakova IN, Patel JR, Rafael-Fortney JA, Ervasti JM. Cytoplasmic gamma-actin contributes to a compensatory remodeling response in dystrophin-deficient muscle. Proc Natl Acad Sci U S A 2006;103:5385–90.

20. Eaton SL, Roche SL, Llavero Hurtado M, et al. Total protein analysis as a reliable loading control for quantitative fluorescent western blotting. PLoS One 2013;8:e72457.

21. Chen B, Guo A, Zhang C, et al. Critical roles of junctophilin-2 in T-tubule and excitation-contraction coupling maturation during postnatal development. Cardiovasc Res 2013;100:54–62.

22. van Oort RJ, Garbino A, Wang W, et al. Disrupted junctional membrane complexes and hyperactive ryanodine receptors after acute junctophilin knockdown in mice. Circulation 2011;123:979–88.

23. Wu CY, Chen B, Jiang YP, et al. Calpain-dependent cleavage of junctophilin-2 and T-tubule remodeling in a mouse model of reversible heart failure. J Am Heart Assoc 2014;3:e000527.

24. Kerr JP, Robison P, Shi G, et al. Detyrosinated microtubules modulate mechanotransduction in heart and skeletal muscle. Nat Commun 2015;6:8526.

25. Williams IA, Allen DG. Intracellular calcium handling in ventricular myocytes from mdx mice. Am J Physiol Heart Circ Physiol 2007;292:H846–55.

26. Wei S, Guo A, Chen B, et al. T-tubule remodeling during transition from hypertrophy to heart failure. Circ Res 2010;107:520–31.

27. Takeshima H, Komazaki S, Nishi M, Iino M, Kangawa K. Junctophilins: a novel family of junctional membrane complex proteins. Mol Cell 2000;6:11–22.

28. Li RC, Tao J, Guo YB, et al. In vivo suppression of microRNA-24 prevents the transition toward decompensated hypertrophy in aortic-constricted mice. Circ Res 2013;112:601–5.

29. Xu M, Wu HD, Li RC, et al. Mir-24 regulates junctophilin-2 expression in cardiomyocytes. Circ Res 2012;111:837–41.

30. Caldwell JL, Smith CE, Taylor RF, et al. Dependence of cardiac transverse tubules on the BAR domain protein amphiphysin II (BIN-1). Circ Res 2014;115:986–96.

KEY WORDS calcium handling, Duchenne cardiomyopathy, junctophilin-2, microtubules

APPENDIX For supplemental figures, please see the supplemental appendix.